

Analysis of the Influence of Thermal Treatment on the Stability of $\text{Ag}_{1-x}\text{Sb}_{1+x}\text{Te}_{2+x}$ and Se-Doped AgSbTe_2

P.M. WYZGA^{1,2} and K.T. WOJCIECHOWSKI¹

1.—Thermoelectric Research Laboratory, Department of Inorganic Chemistry, Faculty of Materials Science and Ceramics, AGH University of Science and Technology, Av. A. Mickiewicza 30, 30-059 Cracow, Poland. 2.—e-mail: pawelwyzga@gmail.com

In order to systematize the knowledge on thermodynamic stability and thermoelectric properties of AgSbTe_2 -based alloys, several experiments examining the influence of thermal treatment on their structural and thermoelectric properties were performed. Samples with a nominal composition of AgSbTe_2 and $\text{AgSbTe}_{1.98}\text{Se}_{0.02}$ were prepared and then annealed in various temperature conditions. It was confirmed that $\text{Ag}_{1-x}\text{Sb}_{1+x}\text{Te}_{2+x}$ (β phase) is the only thermodynamically stable ternary compound in the Ag_2Te - Sb_2Te_3 pseudobinary system. It was also proved that thermal stability of β phase is limited—it slowly decomposes below 633 K. In contrast to some reports, it was also indicated that a small amount of Se does not lead to stabilisation of AgSbTe_2 crystal structure. Despite slow kinetics of the decomposition processes, thermoelectric properties of the material are notably affected by thermal treatment and amount of Ag_2Te precipitations. Maximal ZT value of prepared materials varies from 0.65 at 575 K to 1.07 at 563 K.

Key words: Thermoelectric materials, AgSbTe_2 , thermodynamic stability, thermal treatment, thermoelectric properties, Se doping

INTRODUCTION

AgSbTe_2 is widely known ternary chalcogenide and it has been a subject of numerous studies due to its promising thermoelectric properties: high Seebeck coefficient above $300 \mu\text{V K}^{-1}$ and extremely low thermal conductivity in the range of $0.6\text{--}0.7 \text{ W m}^{-1} \text{ K}^{-1}$.¹ As a result, some authors report very high thermoelectric figure of merit $ZT > 1.4$ for samples with various amount of dopant.^{2–4} AgSbTe_2 is also used as a component of alloys. The AgSbTe_2 alloys with GeTe (so called TAGS) with a maximum value of $ZT_{\text{max}} = 1.5$ at 750 K were considered the best thermoelectric materials for quite a long time.⁵ The PbTe alloys with AgSbTe_2 feature $ZT_{\text{max}} = 2.2$ at 800 K, which is one of the highest reported figures of merit for bulk thermoelectric materials.⁶ However, the application of those alloys seems to be limited as, due to their thermodynamic instability and inhomogeneity, they lose their

excellent thermoelectric properties during long-term annealing at high temperatures.

First experimental results of crystallographic properties of AgSbTe_2 were reported by Geller and Wernick.⁷ They assumed that single crystals prepared by them had rock salt structure ($Fm\bar{3}m$), with Ag and Sb atoms distributed statistically in one of the Wyckoff positions (4a) and Te atoms occupying the second one (4b). Geller and Wernick observed that the nature of the disorder should be complicated because both type of atoms: Ag and Sb differ significantly in electronic structure, atomic radius, and other chemical properties. Therefore, others consider also different probable superstructures, e.g. tetragonal $P4/mmm$ or trigonal $R\bar{3}m$ ⁸ to explain unusual electronic properties of this compound.

The problem of thermodynamic stability of AgSbTe_2 and related alloys was investigated by several groups. Marin-Ayral et al.⁹ and Petzow et al.¹⁰ elaborated independently two slightly different phase diagrams of the pseudobinary Ag_2Te - Sb_2Te_3 system in the same year. Figures 1 and 2

(Received July 18, 2015; accepted September 28, 2015; published online October 27, 2015)

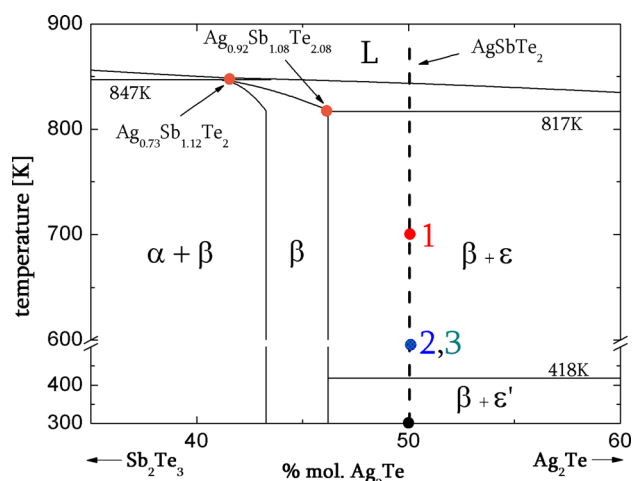


Fig. 1. Part of the phase diagram of $\text{Sb}_2\text{Te}_3\text{-Ag}_2\text{Te}$ pseudobinary system based on Marin-Ayral et al.⁹ Points (1, 2, 3) correspond to temperatures of annealing; alloys with specific chemical composition were marked.

present parts of both diagrams with symbols of main phases normalised by us to facilitate their comparison. Analysing both diagrams, one can easily conclude that a thermodynamically stable compound with nominal composition of AgSbTe_2 indeed does not exist. Authors of both diagrams agreed that β phase with a wide range of compositions ($\text{Ag}_{1-x}\text{Sb}_{1+x}\text{Te}_{2+x}$; $x = 0.06\text{--}0.28$) is the only ternary compound in the $\text{Sb}_2\text{Te}_3\text{-Ag}_2\text{Te}$ system. The β phase has a cubic structure of the hypothetical AgSbTe_2 compound. It should be noted, i.e., that the chemical formula for this phase suggests that Te atoms occupy both sublattices or other structural defects (e.g. vacancies) are present in the crystal structure. Therefore, it seems that the problem of the disorder in this compound is more complicated than that assumed by Geller and Wernick. At this point, it is worth highlighting the typical problem appearing in the literature—several authors tend to identify this phase with stoichiometric AgSbTe_2 . This leads them to misleading experimental methodology and conclusions.

Another problem are doubts concerning the range of stability of the β phase. Following Marin-Ayral et al.,⁹ the β phase exists in a temperature range from 300 K to above 800 K (Fig. 1), which is not coherent with the phase diagram of Petzow et al.¹⁰ Figure 2 shows that at 633 K the process of decomposition of β phase into α (solid solution of Ag in Sb_2Te_3) and ϵ (solid solution of Sb in $\beta\text{-Ag}_2\text{Te}$) solid solutions occurs. Wu et al.¹¹ seem to settle this discrepancy. According to them, annealing at $T = 523$ K leads to the decomposition of β phase, which is not observed after thermal treatment in 673 K.¹¹ Moreover, differential scanning calorimetry (DSC) analyses performed by Wojciechowski et al. also confirm decomposition in 633 K.¹² However, there are still some discrepancies considering

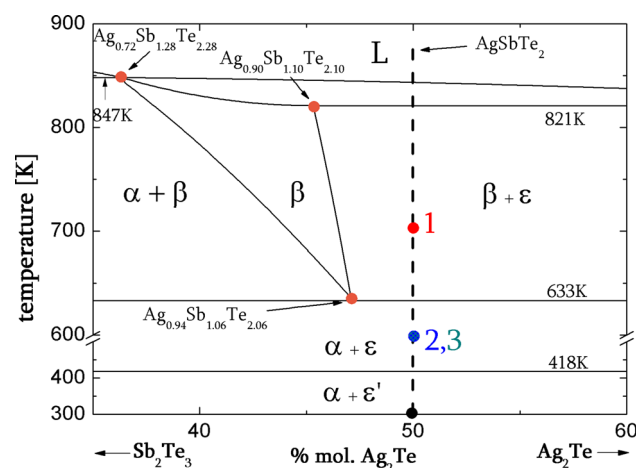


Fig. 2. Part of the phase diagram of $\text{Sb}_2\text{Te}_3\text{-Ag}_2\text{Te}$ pseudobinary system based on Petzow et al.¹⁰ Points (1, 2, 3) correspond to temperatures of annealing; alloys with specific chemical composition were marked.

the existence of α and ϵ solid solutions and the range of existence of β phase.

A crucial problem connected with AgSbTe_2 -based materials is the reproducibility of thermoelectric properties. It was found that electronic properties of these materials, especially the Seebeck coefficient and electrical conductivity, are constantly changing during thermal treatment. Schmidt et al.² reported that alloy with a nominal composition of $\text{AgSbTe}_{1.98}\text{Se}_{0.02}$ exhibits a great deal high ZT of 1.48 at 520 K but after annealing that value decreases to about 0.7 in the same temperature. Although such an effect should be taken into account, there are few articles considering it.^{2,13}

In this study, we have tried to systematize the knowledge on AgSbTe_2 -based materials, revise both phase diagrams^{9,10} and results of structural and thermoelectric measurements presented in the literature.^{2-4,12,14}

EXPERIMENTAL PROCEDURES

One of our aims was to elaborate simple methodology of examination whether selected dopant stabilizes the crystal structure of AgSbTe_2 -based materials. In order to do this, samples with nominal composition of $\text{AgSbTe}_{2-x}\text{Se}_x$ ($x = 0; 0.2$) were prepared by direct melting of elements under vacuum. Elements: Ag (99.99%, Alfa Aesar), Sb (99.99%, Alfa Aesar), Te (99.999%, Alfa Aesar), and Se (99.999%, Alfa Aesar), in the form of small pieces, were weighed and sealed in quartz ampoules under vacuum (<40 Pa). Synthesis was carried out at a temperature of 1023 K for 4 h in a rocking furnace until the alloy was completely melted and homogenised. Then, ampoules were slowly cooled down at a rate below 2 K/min or rapidly quenched by putting them into cold water. Ingots were manually ground in agate mortar and separated into two parts.

The first one was used for x-ray diffraction (XRD, PANalytical Empyrean, Cu K_{α} , without monochromator) and DSC (Netzsch Pegasus 404F3, heating rate: 10 K/min, atmosphere: Ar) measurements, after which samples were sealed in ampoules again and the process of annealing was performed. We have selected three different conditions of annealing: 703 K for 7 days, 523 K for 7 days, 523 K for a month. These conditions were marked on phase diagrams: points 1, 2, and 3, respectively, on Figs. 1 and 2. After each heat treatment, XRD analysis was performed.

The second series of samples was sintered using pulsed electric current sintering (723 K, 5 min, 30 MPa, graphite dies). Obtained cylindrical samples with different height (ca. 10 and 2 mm) were used for measurements of electrical properties and thermal conductivity, respectively. Thermoelectric properties were determined in a temperature range of 323–623 K. Densities of the samples were determined with the use of immersion technique with water as a medium.

Seebeck coefficient and electrical conductivity were determined simultaneously using the DC four-probe method. Thermal diffusivity and specific heat was measured using laser flash method (LFA, Netzsch LFA 457 MicroFlash™, atmosphere: Ar). Dimensionless thermoelectric figure of merit ZT was calculated from Eq. 1:

$$ZT = \frac{\alpha^2 \sigma}{\lambda} T \quad (1)$$

where α —Seebeck coefficient, σ —electrical conductivity, λ —thermal conductivity and T —absolute temperature.

RESULTS AND DISCUSSION

AgSbTe₂ Samples

The first issue we have tried to explain was the influence of the cooling rate of materials just after synthesis on their structural properties. There is a strong conviction in the literature that it is possible to obtain metastable homogeneous AgSbTe₂ only as a result of fast cooling down and quenching of liquid alloy with the same chemical composition.^{2–4,9,11,12,14} However, we have found that XRD patterns of both slowly cooled and quenched samples do not differ substantially (Fig. 3). Analysing the results one can conclude that samples after synthesis contain small amounts of Ag₂Te precipitations. The XRD pattern of this compound is scarcely visible and can be easily overlooked. Significant broadening of Ag₂Te reflections (large FWHM parameter) indicates that the size of crystallites can be in the range of nanometres. We did not observe the presence of the Sb₂Te₃ inclusions. Scanning electron microscopy (SEM) observations confirmed above XRD results. The materials consist of the main, well crystallized phase and lamellar pearlite-like inclusions of Ag₂Te

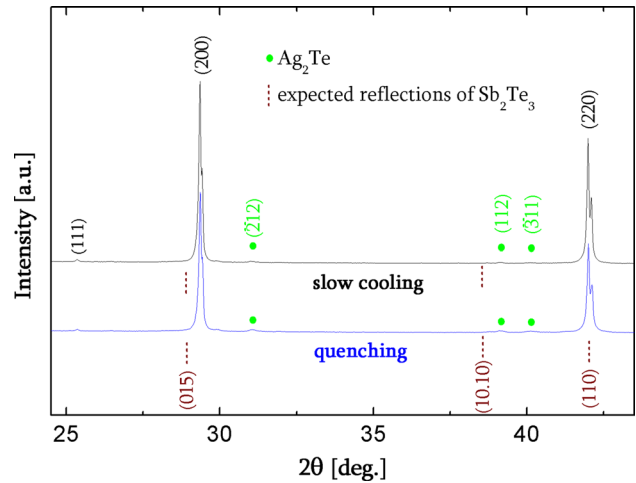


Fig. 3. Enlarged XRD patterns of AgSbTe₂ samples after synthesis with quenching and slow cooling. Positions of expected reflections of Sb₂Te₃ were marked.

dispersed at grain boundaries. The energy dispersive spectroscopy analysis of the main phase shows that it has chemical composition close to Ag_{0.94}Sb_{1.06}Te_{2.06} that corresponds quite well to the composition of the β phase on both cited phase diagrams (Figs. 1 and 2). Summarizing, cooling down the liquid alloy with the nominal composition of AgSbTe₂ leads to the formation of the nonstoichiometric β phase and Ag₂Te despite different rates of cooling applied in our experiments.

The main difference in the cited phase diagrams^{9,10} concerns the range of the existence of the β phase. According to Petzow,¹⁰ it undergoes total decomposition into α and ε below 633 K; on the other hand, Marin-Ayral et al.,⁹ believe that β phase is thermally stable even at room temperature (RT). To verify these discrepancies we have annealed the prepared samples at selected temperatures for the period of 1 week or more. Fig. 4 shows their XRD patterns. We have found that thermal treatment at temperatures above 633 K does not lead to the decomposition of the β phase. The samples annealed below this temperature slowly decomposes into Sb₂Te₃ and Ag₂Te. However, the kinetics of this process can be very slow. For example, the XRD pattern of the sample annealed at 523 K does not differ notably from the pattern of the pure β phase. The significant amounts of Sb₂Te₃ and Ag₂Te are clearly visible after 1 month of thermal treatment at this temperature. Our experiment confirms validity of phase diagrams elaborated by Petzow et al.¹⁰ and Wu et al.¹¹

DSC analysis of the samples was performed in order to identify temperatures of phase transitions (Fig. 5). During the first DSC measurement of quenched and slowly cooled samples, a small peak around 418 K can be observed. We associate it with the ε' – ε phase transition of Ag₂Te. That small endothermic effect vanishes after cooling. Rapid

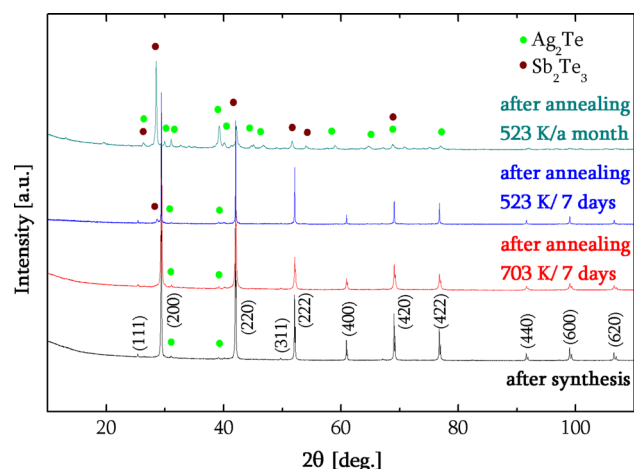


Fig. 4. XRD patterns of AgSbTe_2 samples after synthesis and annealing.

cooling inhibits also the decomposition of β phase; therefore, the peak at 633 K is not detected during the first DSC measurement of the quenched sample. However, the second DSC run shows the presence of the large endothermic peak at about 630 K which is clearly related to synthesis of β phase from ε and α phases. This means that the quenched sample has decomposed during slow cooling ($\Theta < 5$ K/min) of the DSC apparatus after first measurement. It should be noted that this endothermic peak is always visible on DSC curves of slowly cooled samples. At the same time, there are no XRD patterns corresponding to α phase for these samples. The reason might be similar to Ag_2Te —the amount of α phase (Sb_2Te_3) is small and it may be in the form of nanosized crystallites; therefore, possible reflections are invisible and probably broadened. Moreover, position of the reflection with maximal intensity for Sb_2Te_3 ($28,238^\circ$) is close to analogous reflection for AgSbTe_2 phase ($29,356^\circ$), so they might be overlapped. A small endothermic effect around 600 K, visible on selected curves, might be connected with creation of Ag_5Te_3 .⁹ These conclusions are partially coherent with the study of Du et al.¹⁴

Electrical properties were measured twice in heating and cooling modes. Figure 6 presents electrical conductivity as a function of temperature. Temperature dependence of electrical conductivity suggest metal-like properties of the studied materials. For each subsequent stage of measurements, electrical conductivity gradually increases and finally reaches $1.5 \times 10^4 \text{ S m}^{-1}$ at 323 K. Moreover, temperature dependencies of electrical conductivity during heating and cooling mode differ significantly what can suggest that some phase transition occurs during measurements. Sudden changes in electrical properties take place close the temperature of 405 K, which corresponds to ε' - ε transition of Ag_2Te (Fig. 6, solid line). Temperature dependencies of either electrical conductivity or Seebeck coefficient

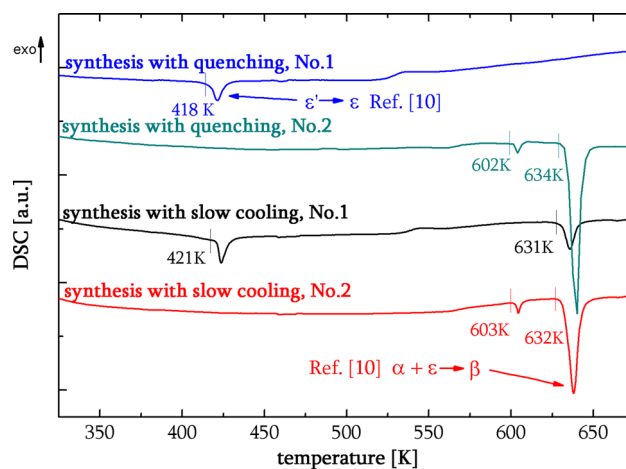


Fig. 5. DSC curves of AgSbTe_2 samples (heating rate 10 K/min and sample mass ca. 10 mg). Nos. 1 and 2 indicate the first and the second measurement, respectively.

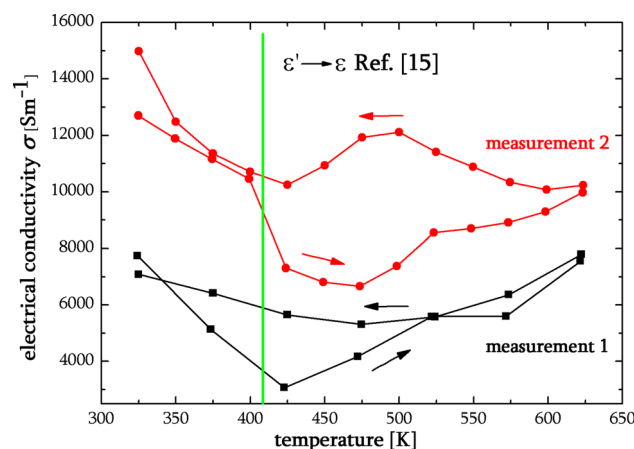


Fig. 6. Temperature dependence of electrical conductivity of AgSbTe_2 sample. Solid line corresponds to the temperature of the ε' - ε phase transition of Ag_2Te .

are very similar to those measured for pure Ag_2Te , reported by Ragimov et al.¹⁵ Therefore, we conclude that the presence of Ag_2Te strongly affects electrical properties of the materials.

Prepared samples exhibit p -type conductivity within the entire temperature range. Maximal value of Seebeck coefficient for obtained samples is equal to $270 \mu\text{V K}^{-1}$ at 574 K in the second measurement cycle (Fig. 7). The temperature dependencies of Seebeck coefficient reflects changes in electrical conductivity, but the value of thermopower decreases systematically from one measurement to another.

Thermal conductivity was evaluated indirectly using LFA method. Figure 8 shows that the measured samples exhibit extremely low thermal conductivity ca. $0.7 \text{ W m}^{-1} \text{ K}^{-1}$ within the entire range of measurements. That phenomena was discussed by Morelli et al.¹ on the basis of different scattering mechanisms of phonons. No influence of the phase

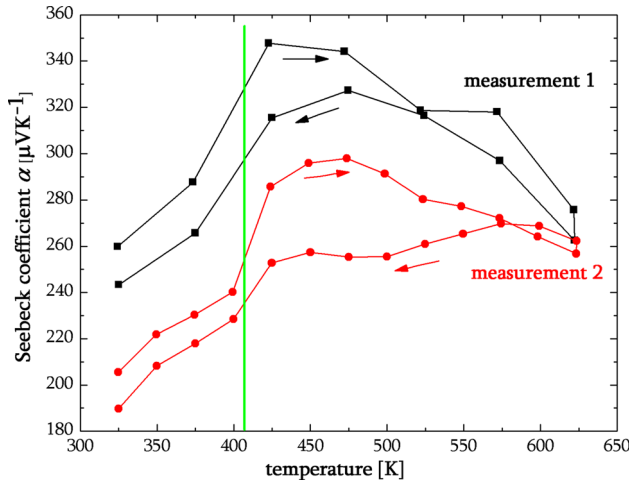


Fig. 7. Temperature dependence of Seebeck coefficient of AgSbTe_2 sample. Solid line as on previous figure.

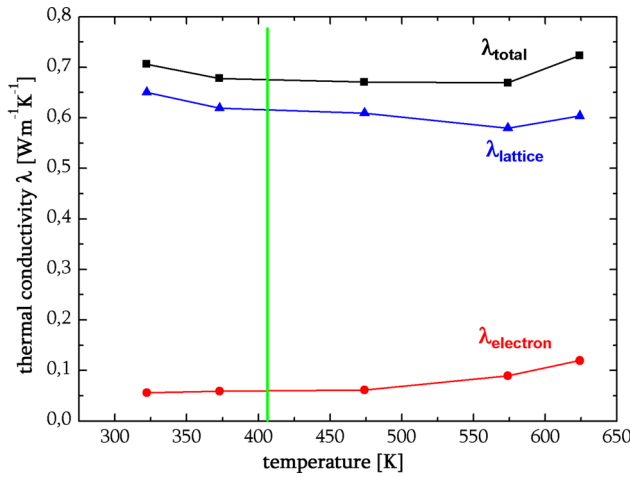


Fig. 8. Temperature dependence of thermal conductivity of AgSbTe_2 sample. Solid line as on previous figure.

transition of Ag_2Te on thermal conductivity is observed. Nevertheless, lamellar precipitations of Ag_2Te are believed to play a crucial role in phonon scattering.^{16,17}

Dimensionless thermoelectric figure of merit ZT was calculated for obtained material (Eq. 1). Values of ZT gradually grow due to a high increase in electrical conductivity, even compensating for a drop of Seebeck coefficient (Fig. 9). The highest experimental value reaches 0.65 at 575 K for the second measurement cycle. The form of the curves relates to hysteresis presented in prior figures. Results are comparable with some of the reported data^{2,12} and slightly lower than those determined by Du et al.³ Discrepancies might be induced mostly by instability of β phase. Despite relatively slow kinetics of the process of decomposition, illustrated by x-ray analysis (Fig. 4), changes in thermoelectric properties of obtained material are notable.

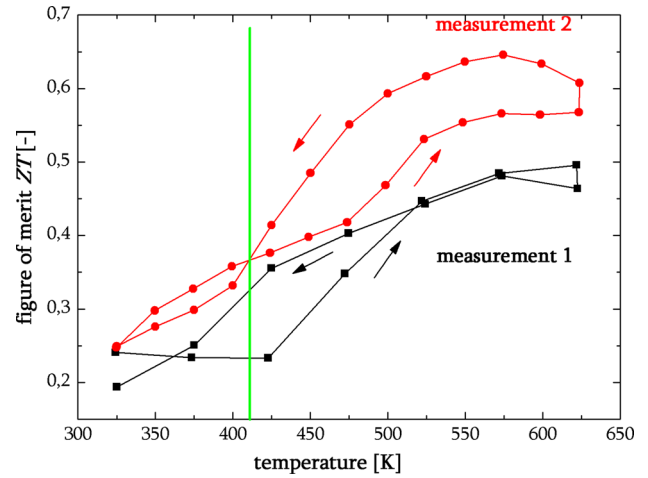


Fig. 9. Temperature dependence of the figure of merit ZT of the AgSbTe_2 sample. Solid line as on previous figure.

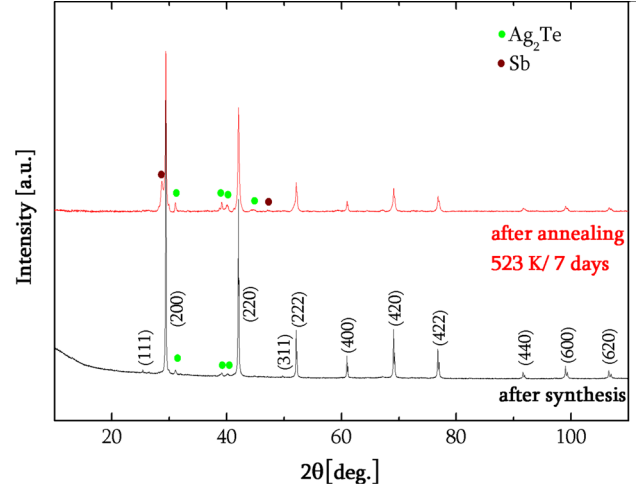


Fig. 10. XRD pattern of $\text{AgSbTe}_{1.98}\text{Se}_{0.02}$ samples after synthesis and annealing.

$\text{AgSbTe}_{1.98}\text{Se}_{0.02}$ Samples

Because of the very attractive thermoelectric properties of quenched AgSbTe_2 alloys, some authors made attempts to stabilize their structure by doping with small amounts of various elements, including Se.^{2-4,12} For example, Du et al.,³ reported that even small amount of Se leads to the stabilization of the crystal structure of stoichiometric AgSbTe_2 . It is not consistent with the work of Wojciechowski et al.,¹² who report that $\text{AgSbTe}_{2-x}\text{Se}_x$ solid solutions are stable at RT only for $x > 1$. Similar results are reported by Wu et al.⁴: for $x < 1$, samples consist of at least two phases. To revise the opposite conclusions on thermodynamic stability of Se doped material, we have repeated the research methodology applied for AgSbTe_2 samples.

XRD patterns of Se doped samples are similar to those of undoped AgSbTe_2 sample (Fig. 10). There

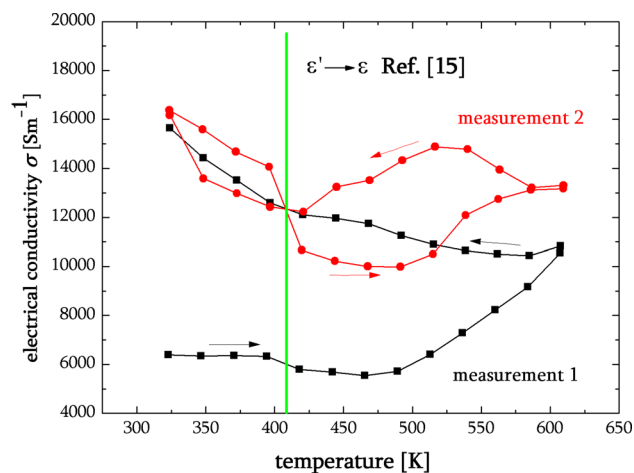


Fig. 11. Temperature dependence of electrical conductivity of $\text{AgSbTe}_{1.98}\text{Se}_{0.02}$ sample. Solid line corresponds to the temperature of the ϵ' – ϵ phase transition of Ag_2Te .

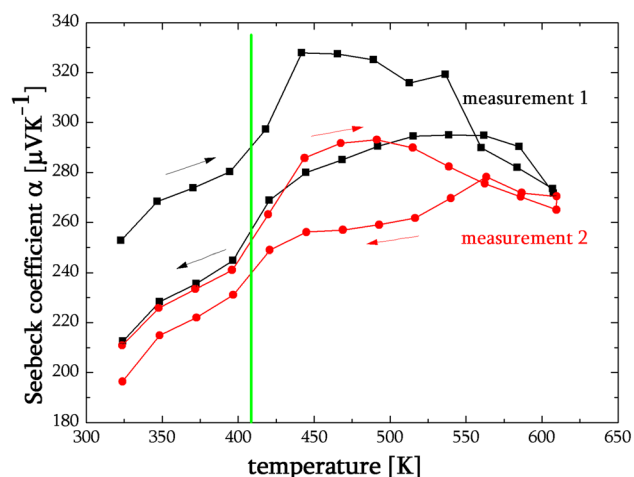


Fig. 12. Temperature dependence of Seebeck coefficient of $\text{AgSbTe}_{1.98}\text{Se}_{0.02}$ sample. Solid line as on previous figure.

are no visible reflections corresponding to Se-based phases and small shifts in pattern positions when compared with the AgSbTe_2 sample, as is noted. This proves that the process of introducing Se into the crystal lattice was successfully accomplished. On the other hand, precipitations of Ag_2Te were found in the material, which demonstrates lack of thermodynamic stability of the alloy with nominal composition of $\text{AgSbTe}_{1.98}\text{Se}_{0.02}$. Furthermore, patterns related to Sb occurs after thermal treatment.

Electrical properties of $\text{AgSbTe}_{1.98}\text{Se}_{0.02}$ sample are presented in the Figs. 11 and 12. Either electrical conductivity or Seebeck coefficient exhibit the same temperature dependencies as observed for the previous AgSbTe_2 samples. Electrical conductivity increases slightly after doping, reaching $1.6 \times 10^4 \text{ S m}^{-1}$ at 323 K. The hysteresis-like character is invariably visible in that dependence. AgSb-

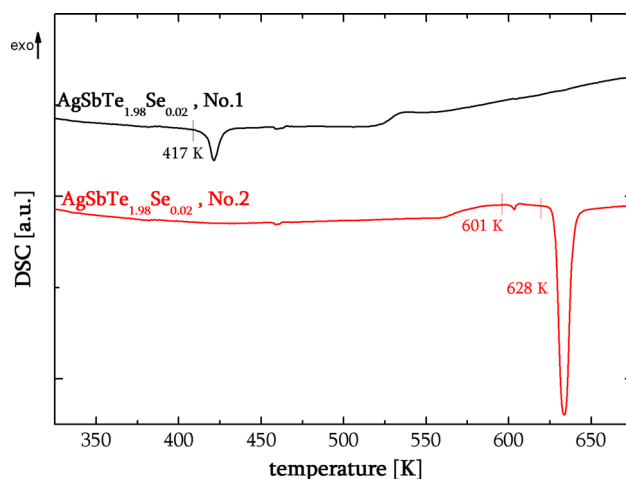


Fig. 13. DSC curves of $\text{AgSbTe}_{1.98}\text{Se}_{0.02}$ samples (heating rate 10 K/min and samples mass ca. 10 mg). Nos. 1 and 2 indicate the first and the second measurement, respectively.

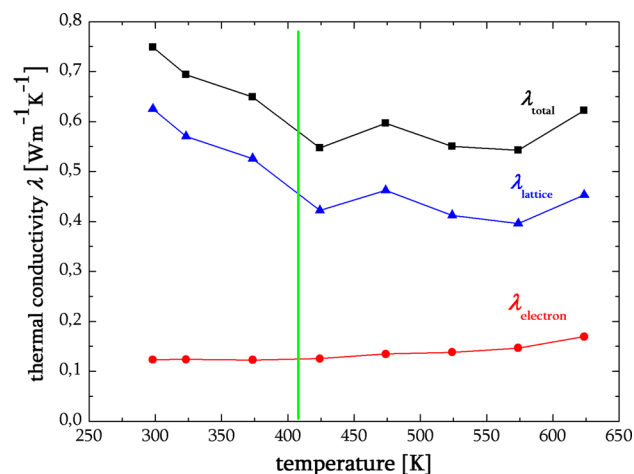


Fig. 14. Temperature dependence of thermal conductivity of $\text{AgSbTe}_{1.98}\text{Se}_{0.02}$ sample. Solid line as on previous figure.

$\text{Te}_{1.98}\text{Se}_{0.02}$ is *p*-type semiconductor and has Seebeck coefficient similar to undoped AgSbTe_2 sample: maximal value of $278 \mu\text{V K}^{-1}$ was measured at 563 K. The influence of Ag_2Te precipitations on transport properties is directly visible and the temperature of ϵ' – ϵ phase transition of Ag_2Te was marked (solid line).

Summarizing, one can conclude that Se-doped β phase is not thermally stable. Both structural and thermoelectric studies indicate that the process of decomposition occurs in the material. Such outcome does not harmonize with the study of Du et al.,³ who claims that introducing small amounts of Se results in the stabilisation of the crystal structure of the AgSbTe_2 compound. On the contrary, this confirms the research of Schmidt et al.,² who observed the decomposition of $\text{AgSbTe}_{2-x}\text{Se}_x$ materials. DSC measurements are also comparable with those of AgSbTe_2 samples (Fig. 13).

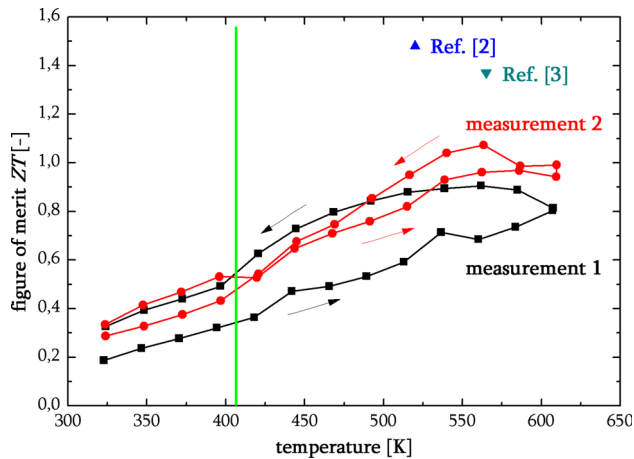


Fig. 15. Temperature dependence of the figure of merit ZT of $\text{AgSbTe}_{1.98}\text{Se}_{0.02}$ sample. Solid line as on previous figure.

Thermal conductivity does not differ notably from those of AgSbTe_2 sample. $\text{AgSbTe}_{1.98}\text{Se}_{0.02}$ shows minimum value of thermal conductivity of $0.55 \text{ W m}^{-1} \text{ K}^{-1}$ at 424 K. Lattice contribution constantly plays the main role in heat transfer through the material, whereas increase in electrical component is observed as a result of the growth of electrical conductivity (Fig. 14).

Calculated ZT values exhibit enhancement, comparing with AgSbTe_2 sample (Fig. 15). Maximal value equals 1.07 at 563 K, which is somewhat lower than in related studies.^{2,3} Thermal treatment leads to the increase of the ZT parameter mostly affected by electrical conductivity. However, decomposition of $\text{AgSbTe}_{1.98}\text{Se}_{0.02}$ alloy is visible and it is no longer homogenous material.

CONCLUSIONS

Samples with nominal composition of AgSbTe_2 and $\text{AgSbTe}_{1.98}\text{Se}_{0.02}$ were obtained and the influence of thermal treatment on their structural, thermal, and thermoelectric properties from RT to 625 K were studied. After synthesis, AgSbTe_2 decomposes to a nearly homogenous main β phase with chemical composition of $\text{Ag}_{1-x}\text{Sb}_{1+x}\text{Te}_{2+x}$ ($x \sim 0.06\text{--}0.1$) and Ag_2Te precipitations. We have confirmed that the β phase is the only stable ternary phase in the $\text{Sb}_2\text{Te}_3\text{--Ag}_2\text{Te}$ system. Moreover, this phase slowly decomposes into Ag_2Te and Sb_2Te_3 below 633 K. Results are in line with the phase diagram given by Petzow et al.¹⁰ and contradict the phase diagram of Marin-Ayral et al.⁹

All specimens are p -type semiconductors. Temperature dependencies of thermoelectric properties of all samples are strongly affected by the presence of Ag_2Te precipitations. Sharp change, especially in the case of electrical conductivity and Seebeck coefficient, in approximately 405 K is strictly related to the $\epsilon'\text{--}\epsilon$ phase transition of Ag_2Te .

$\text{AgSbTe}_{1.98}\text{Se}_{0.02}$ exhibits enhanced thermoelectric properties, but not as high as previously re-

ported values.^{2,3} Using the same methodology applied for AgSbTe_2 , we have shown that this compound also slowly decomposes into Sb_2Te_3 and Ag_2Te . High reported values of $ZT \sim 1.4\text{--}1.6$ can be an artefact as a result of structural changes in measurement conditions.

Investigation of AgSbTe_2 -based alloys leads to the conclusion that the properties of materials within the Ag-Sb-Te system are strongly influenced by thermal treatment and should be routinely analyzed in more than one measurement cycle. Applied methodology of the experiment can be successfully used for the examination of thermodynamic stability of AgSbTe_2 -based materials.

ACKNOWLEDGEMENTS

This work was supported by the funds of National Science Center granted on the basis of the decision No. DEC-2013/09/B/ST8/02043.

OPEN ACCESS

This article is distributed under the terms of the Creative Commons Attribution 4.0 International License (<http://creativecommons.org/licenses/by/4.0/>), which permits unrestricted use, distribution, and reproduction in any medium, provided you give appropriate credit to the original author(s) and the source, provide a link to the Creative Commons license, and indicate if changes were made.

REFERENCES

1. D.T. Morelli, V. Jovovic, and J.P. Heremans, *Phys. Rev. Lett.* 101, 035901 (2008).
2. M. Schmidt and K.T. Wojciechowski, *AIP Conf. Proc.* 1449, 175 (2012).
3. B. Du, H. Li, J. Xu, X. Tang, and C. Uher, *Chem. Mater.* 22, 5521 (2010).
4. H.-J. Wu, T.-W. Lan, S.-W. Chen, Y.-Y. Chen, T. Day, and G.J. Snyder, *Acta Mater.* 93, 38 (2015).
5. A.Q. Morrison, E.D. Case, F. Ren, A.J. Baumann, D.C. Kleinow, J.E. Ni, T.P. Hogan, J. D'Angelo, N.A. Matchanov, T.J. Hendricks, N.K. Karri, C. Cauchy, J. Barnard, and M.G. Kanatzidis, *Mater. Chem. Phys.* 134, 973 (2012).
6. K.F. Hsu, S. Loo, F. Guo, W. Chen, J.S. Dyck, C. Uher, T. Hogan, E.K. Polychroniadis, and M.G. Kanatzidis, *Science* 5659, 818 (2004).
7. S. Geller and J.H. Wernick, *Acta Cryst.* 12, 46 (1959).
8. E. Quarez, K.F. Hsu, R. Pcionek, N. Frangis, E.K. Polychroniadis, and M.G. Kanatzidis, *J. Am. Chem. Soc.* 127, 9177 (2005).
9. R.M. Marin-Ayral, B. Legendre, G. Brun, B. Liautard, and J.C. Tedenac, *Thermochim. Acta* 131, 37 (1988).
10. G. Petzow and G. Effenberg, *Ternary Alloys*, Vol. 2 (Weinheim: Wiley, 1988), p. 554.
11. H.-J. Wu and S.-W. Chen, *Acta Mater.* 59, 6463 (2011).
12. K.T. Wojciechowski and M. Schmidt, *Phys. Rev. B* 79, 184202 (2009).
13. Z. He, L. Jun, Z. Hang-Tian, L. Quan-Lin, L. Jing-Kui, L. Jing-Bo, and L. Guang-Yao, *Chin. Phys. B* 21, 106101 (2012).
14. B. Du, Y. Yan, and X. Tang, *J. Electron. Mater.* 44, 6 (2015).
15. S.S. Ragimov and S.A. Aliev, *Inorg. Mater.* 43, 1184 (2007).
16. J.D. Sugar and D.L. Medlin, *J. Alloy. Compd.* 478, 75 (2009).
17. H.-J. Wu and S.-W. Chen, *J. Alloy. Compd.* 509, 656 (2011).